■ **Fluorescent Probes** |*Hot Paper*|

A Systematic Study of Coumarin–Tetrazine Light-Up Probes for Bioorthogonal Fluorescence Imaging

Juraj Galeta, Rastislav Dzijak, Jan Obořil, Martin Dračínský, and Milan Vrabel*[a]

Abstract: Fluorescent probes that light-up upon reaction with complementary bioorthogonal reagents are superior tools for no-wash fluorogenic bioimaging applications. In this work, a thorough study is presented on a set of seventeen structurally diverse coumarin–tetrazine probes that produce fluorescent dyes with exceptional turn-on ratios when reacted with *trans*-cyclooctene (TCO) and bicyclononyne (BCN) dienophiles. In general, formation of the fully aromatic pyridazine-containing dyes resulting from the reaction with

BCN was found superior in terms of fluorogenicity. However, evaluation of the probes in cellular imaging experiments revealed that other factors, such as reaction kinetics and good cell permeability, prevail over the fluorescence turn-on properties. The best compound identified in this study showed excellent performance in live cell-labeling experiments and enabled no-wash fluorogenic imaging on a timescale of seconds.

Introduction

Fluorescent labeling of biomolecules based on selective chemical reactions is an important strategy used to interrogate and study biological processes.[1] The ever-growing arsenal of fluorescent dyes provides us with a set of tools fitting different applications.[2] A good signal-to-noise ratio is one of the fundamental requirements to guarantee production of good quality and reliable data in bioimaging experiments.[3] Fluorescent probes that light-up in response to specific activation play a very important role in this regard.[4] In combination with fast reaction kinetics of certain bioorthogonal reactions, these fluorogenic probes have opened up the possibility to analyze and manipulate biological systems with unprecedented precision.[5]

The excellent reactivity of 1,2,4,5-tetrazines with strained dienophiles together with the unique photophysical properties of the tetrazine heterocyclic core led to the development of various fluorogenic probes based on these reaction partners.[6] The ability of tetrazines to quench the fluorescence of certain fluorophores has been first recognized by the Weissleder

group.[7] Since then, the concept has been extended to include BODIPY,[8] xanthene,[9] cyanine[10] and coumarin[11] dyes. Beside these "classical" chromophores, other scaffolds have been exploited for the generation of fluorogenic probes as well.[12] We and others have found that by employing a specific type of dienophiles, it is even possible to generate fluorescent dihydropyridazine dyes directly from non-fluorescent tetrazines.[13]

The mechanism responsible for quenching the fluorescence of tetrazine-modified dyes typically involves FRET (Förster resonance energy transfer), TBET (through-bond energy transfer) or PET (photoinduced electron transfer).[6a] For the FRET mechanism, the emission of the attached fluorophore must match with the absorption band of the tetrazine (usually 520–540 nm). This is not required for TBET-based fluorogenic probes. Together with the PET-based quenching mechanism, this opens up the possibility to generate fluorogenic dyes based on fluorophores emitting in the red-to-near-infrared region.[9c,d,10]

Among the different quenching strategies discussed above, the TBET-based tetrazine probes usually produce the best fluorescence turn-on response in reaction with various dienophiles: a range of several thousand-fold has been reported in the literature.[8a,11] Among these, a series of coumarin-based tetrazines, termed HELIOS probes, showed up to 11 000-fold enhancement in the fluorescent signal in the reaction with TCO dienophiles.[11] These values exceed all other tetrazine-based fluorogenic probes reported to date. Despite these impressive properties, there is no systematic study on such probes available.

To fill this gap, we report here a systematic investigation on the influence of various substituents on the photophysical properties of dyes formed when various coumarin–tetrazines (Coum-Tz) react with two different strained dienophiles, the TCO and BCN (Scheme 1). We further evaluate the light-up

[a] Dr. J. Galeta, Dr. R. Dzijak, J. Obořil, Dr. M. Dračínský, Dr. M. Vrabel
Institute of Organic Chemistry and Biochemistry
Czech Academy of Sciences
Flemingovo nám. 2, 166 10, Prague (Czech Republic)
E-mail: vrabel@uochb.cas.cz

Supporting information and the ORCID identification number(s) for the author(s) of this article can be found under:
https://doi.org/10.1002/chem.202001290

Part of a Special Collection to commemorate young and emerging scientists. To view the complete collection, visit: Young Chemists 2020.
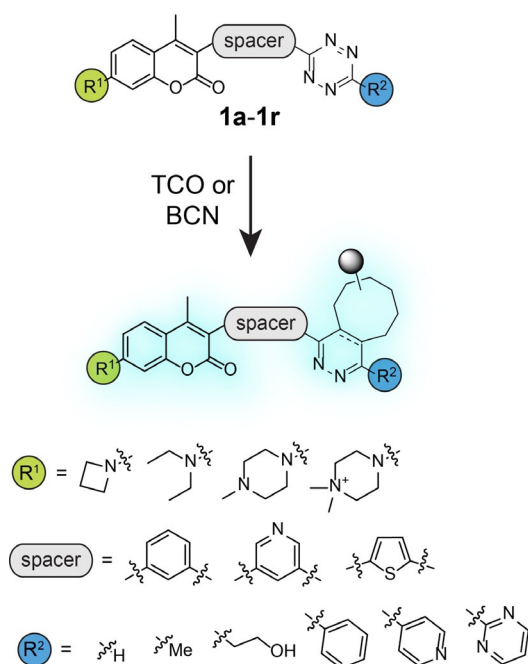
Scheme 1. General formula of coumarin–tetrazine probes and schematic presentation of their fluorogenic reaction with two different dienophiles investigated in this study.

probes in cell imaging experiments and demonstrate their utility for bioorthogonal fluorescence labeling.

Results and Discussion

Synthesis of Coum-Tz probes

To obtain a set of Coum-Tz compounds, we first prepared triflate **2** as a common precursor (Scheme 2). Triflate **2** undergoes high-yielding (>80%) Buchwald–Hartwig cross-coupling reaction with azetidine hydrochloride (usually a much more expensive free base is used). We also prepared N-methylpiperazinyl derivative **3b** with a simple nucleophilic substitution in hot anhydrous 1,4-dioxane. Then, a surprisingly selective and high yielding bromination with NBS in MeCN was performed. We noticed that it is important to dissolve the starting coumarin before NBS addition, otherwise the regioselectivity is poor.

The subsequent Suzuki coupling reactions with various boronic acids were all practical giving high yields, however, 5-cyanothiophene-2-boronic acid required reaction in anhydrous 1,4-dioxane and provided the best result under these conditions (see Supporting Information). All other substrates were also viable except for those containing a dimethylphenyl (**5c**) and thiophene (**5h**) spacer. We did not optimize these two reactions although several attempts were carried out. We note that we also used Heck cross-coupling to obtain the respective alkenyl-substituted tetrazines.[9a] Although the synthesis was viable, the resulting compounds were poorly soluble so were not investigated further. Coumarins **5a**–**h** were then submitted to the final synthetic step with the corresponding nitriles in the presence of Zn(OTf)$_2$ and an excess of hydrazine monohy-

drate at 70 °C. In the case of H-tetrazine (**1d**), we used a recently reported protocol.[14] In this case we got the lowest yield (12%), but typically the compounds can be obtained in 20–30% yield. In general, the preparation of tetrazines with the phenyl spacer was superior over other different spacers, but the character of the partner nitrile also plays an important role. It seems that the pyridinyl spacer is problematic during the oxidation of intermediate dihydrotetrazines using a NaNO$_2$/2 M HCl mixture. In this case the pH must remain above ≈3.
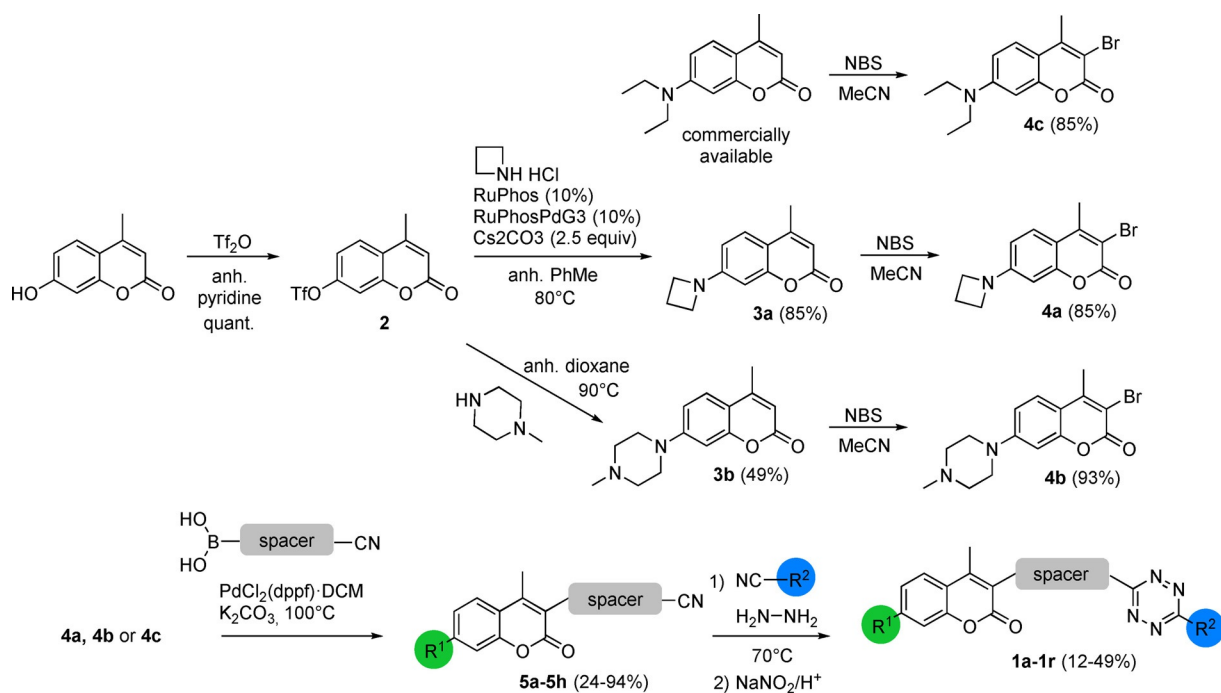
Photophysical properties of the click products

With the pool of seventeen derivatives in hand, we next characterized the photophysical properties of dyes formed when Coum-Tz **1a**–**q** reacted with two different dienophiles (Figure 1). We used the axial isomer of (E)-cyclooct-4-enol (axial TCO-OH) and ((1R,8S,9S)-bicyclo[6.1.0]non-4-yn-9-yl)methanol (endo BCN), which both efficiently react with tetrazines, but differ in the reaction products. While the axial TCO-OH leads to the formation of 1,4-dihydropyridazine, BCN yields fully aromatic pyridazines. Previous studies on fluorogenic tetrazines based on fluorescein, rhodamine and bodipy fluorophores showed better turn-on ratios for dyes containing the fully aromatic pyridazine moiety.[9a, 15] Since no such data are available for fluorogenic coumarin dyes, we were interested in seeing how the formation of dihydropyridazines vs. pyridazines would influence the photophysical properties of the resulting dyes.

As already mentioned in the original study of the Weissleder group, very high purity of the starting tetrazines is required to ensure good fluorescence turn-on ratios.[11] The same was true in our hands and we found that even traces of impurities can cause an order of magnitude difference in the determined fluorescence turn-on ratios (Figure S2). We therefore purified all the Coum-Tz conjugates by analytical HPLC prior to the fluorescence turn-on measurements. The freshly purified tetrazines were then mixed with an excess of the respective dienophile to initiate the fluorogenic reaction. As expected, we observed significant fluorescence turn-on ratios ranging from 40-fold to an impressive 5000-fold (Table 1, Table S1 and Figure S4). The large set of the Coum-Tz probes used in this study allow us to draw the following general conclusions. Our data

Milan Vrabel studied chemistry at the Slovak University of Technology in Slovakia, where he obtained his diploma in 2004. He then moved to the Institute of Organic Chemistry and Biochemistry (IOCB) in Prague, where he worked with Prof. M. Hocek and obtained his Ph.D. in 2008. He then joined the Carell group at the Ludwig-Maximilians University in Munich as a PostDoc. Since 2014, he is a junior group leader at IOCB in Prague, where he works on the development and applications of bioorthogonal reactions. In 2016, he was awarded an ERC Starting Grant for a project that aims to develop new tools in glycobiology.

Chemistry–A European Journal

Full Paper
doi.org/10.1002/chem.202001290

Chemistry
Europe
European Chemical
Societies Publishing

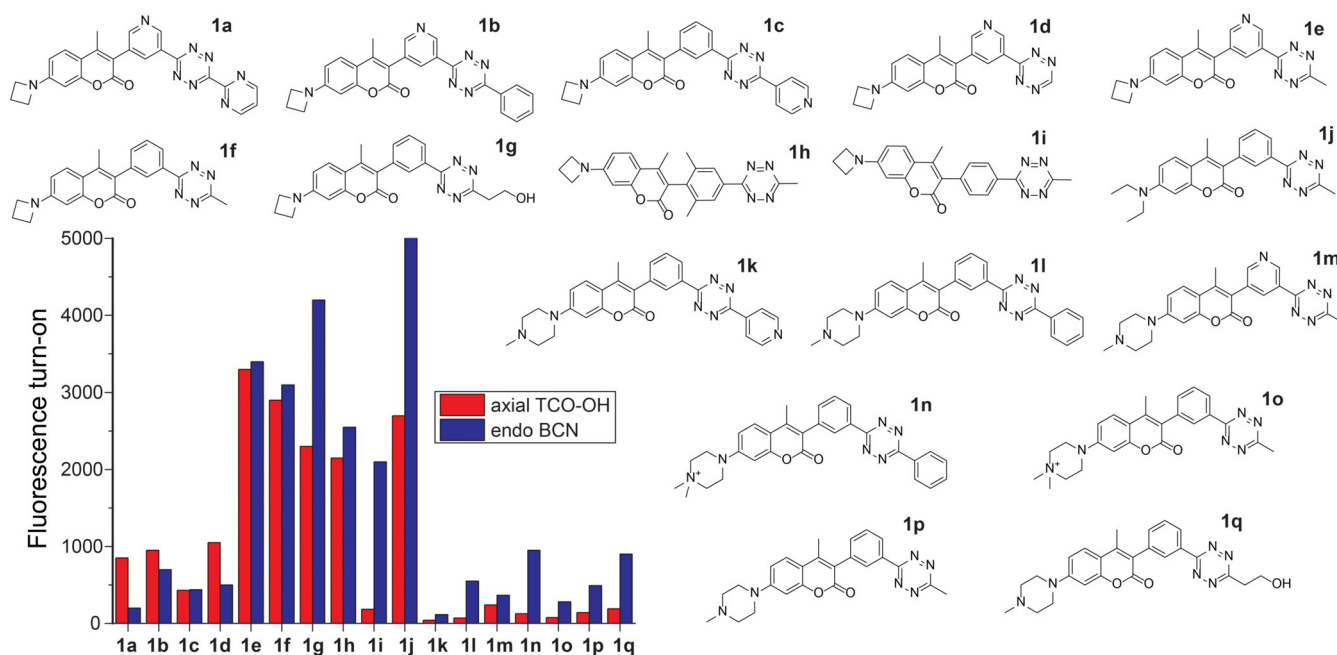**Scheme 2.** Synthesis of Coum-Tz probes.

Figure 1. Structures of the Coum-Tz probes and graph showing summary of the fluorescence turn-on values of the click products formed in the reaction of the probes with the axial TCO-OH and *endo* BCN dienophiles.

show that the dyes formed in the reaction with the *endo* BCN dienophile gave higher turn-on ratios when compared to products formed in the reaction with the axial TCO in most cases. However, this phenomenon strongly depends on the substituents. For example, tetrazine **1a** gave a 4 times stronger signal with the axial TCO when compared to the BCN. The opposite is true for derivatives **1i**, **1n** or **1q**, which all produce brighter dyes with BCN. Our data also show that the presence of an ar-

omatic moiety at position 6 of the tetrazine core (pyrimidyl, phenyl or pyridyl) leads to lower fluorescence turn-on ratios. Derivatives giving the best fluorescence turn-on ratio with both dienophiles all contain alkyl substituent at position 6 (**1e–j**).

In general, the azetidine-substituted coumarin derivatives perform better when compared to derivatives containing the methylpiperazine or *N,N*-dimethylpiperazin-1-ium moiety espe-

Table 1. Photophysical properties of the click products.

Tetrazine	Dienophile	λ_{Abs} [nm][a]	λ_{Em} [nm][a]	ε [M^{-1} s^{-1}][b]	Φ[c]	Fluorescence enhancement
1 a	axial TCO-OH	375	485	11 000	–	850-fold
	endo BCN	375	470	14 000	0.032	200-fold
1 b	axial TCO-OH	381	475	21 600	–	950-fold
	endo BCN	383	455	17 000	–	700-fold
1 c	axial TCO-OH	375	472	27 500	–	430-fold
	endo BCN	370	455	20 000	–	440-fold
1 d	axial TCO-OH	371	485	8 500	–	1050-fold
	endo BCN	371	480	11 500	0.15	500-fold
1 e	axial TCO-OH	370	485	23 000	–	3300-fold
	endo BCN	372	475	22 000	–	3400-fold
1 f	axial TCO-OH	374	483	16 000	–	2900-fold
	endo BCN	376	472	21 000	0.67	3100-fold
1 g	axial TCO-OH	363	483	18 000	–	2300-fold
	endo BCN	365	479	20 000	0.57	4200-fold
1 h	axial TCO-OH	370	475	13 000	–	2200-fold
	endo BCN	382	473	15 500	–	2500-fold
1 i	axial TCO-OH	375	482	16 000	–	190-fold
	endo BCN	367	471	8 600	–	2100-fold
1 j	axial TCO-OH	398	481	12 000	–	2700-fold
	endo BCN	397	463	15 000	0.22	5000-fold
1 k	axial TCO-OH	350	461	6 000	–	40-fold
	endo BCN	348	453	7 000	–	115-fold
1 l	axial TCO-OH	340	460	3 100	–	70-fold
	endo BCN	352	451	10 500	0.38	550-fold
1 m	axial TCO-OH	355	459	29 500	–	240-fold
	endo BCN	355	461	20 000	–	370-fold
1 n	axial TCO-OH	352	457	18 000	–	125-fold
	endo BCN	350	452	25 000	0.58	950-fold
1 o	axial TCO-OH	351	458	21 000	–	75-fold
	endo BCN	351	456	22 500	–	280-fold
1 p	axial TCO-OH	350	459	18 500	–	140-fold
	endo BCN	350	458	17 500	–	490-fold
1 q	axial TCO-OH	353	457	25 500	–	190-fold
	endo BCN	353	457	22 000	–	900-fold

[a] determined in PBS buffer (pH 7.4) except for **1 a**, **b**, **c** and **1 i** where 5 %DMSO in PBS was used instead. [b] at 370 nm in PBS. [c] determined using 370 nm excitation in PBS and using quinine sulfate in H$_2$SO$_4$ (0.5 M, F = 0.55) as the standard.

cially with the axial TCO. The latter compounds also have blue-shifted absorption maxima centered around 350 nm, while the azetidine-substituted coumarins have absorption maxima at around 370 nm (Table 1, Figure S4). We would like to point out that the two *N,N*-dimethylpiperazin-1-ium-substituted derivatives (**1 n** and **1 o**) decompose over time in the solid state as well as in solution (Figure S6). Although we could synthesize, isolate and purify the compounds for the fluorescence light-up measurements, from a practical standpoint, these derivatives were omitted from further experiments.

In a recent study,[16] we demonstrated that the attachment of pyridinium moiety to 1,2,4-triazines can yield fluorogenic compounds having interesting properties. Among other, the compounds were better water soluble and showed organelle-specific accumulation. Introduction of alkylated hetaryl substituents to coumarin fluorophores can significantly influence their photophysical properties and was also used recently to generate redshifted photocages.[17] We thought that similar strategy could be used for the Coum-Tz probes. We have therefore investigated the possibility to alkylate the pyridyl moiety of compounds **1 b** and **1 c**. The alkylation was performed by using dimethylsulfate in DMF. Based on HPLC/MS analysis, the reaction was successful. Unfortunately, the resulting compounds were unstable and could not be practically handled.

In an effort to further extend the structural space of the Coum-Tz compounds, we have also introduced thiophene moiety as the spacer between the coumarin and the tetrazine core (**1 r**). Although the synthesis of this derivative was more complicated when compared to other compounds, we could isolate the compound in reasonable yield (see Supporting Information). However, we did not observe any light-up properties of **1 r** with the TCO or BCN dienophiles and therefore, we did not include this compound in further studies.

During fluorescence spectra acquisition, we unexpectedly observed significant decrease in the signal intensity for many of the tetrazine derivatives with the axial TCO at later time points (Figure S5). This was especially apparent for compounds containing the alkyl substituents. We showed in several earlier studies that the dihydropyridazine isomers (1,4 vs. 4,5) formed in the reaction of tetrazines with different TCOs can be utilized for the formation of fluorophores and that the photophysical

Chemistry–A European Journal

Full Paper
doi.org/10.1002/chem.202001290

Chemistry Europe
European Chemical
Societies Publishing

properties of the dyes depend on the structure of the dihydro-pyridazine core.[13a,c] The axial TCO-OH that we used in this study is able to intramolecularly promote tautomerization of the initially formed 4,5-dihydropyridazine to the respective 1,4-dihydropyridazine. The rate of tautomerization depends on the structure of the tetrazine as well as on the reaction conditions. This has been nicely demonstrated by the ability of structurally different tetrazines to promote the click-to-release reaction, in which the tautomerization plays an essential role.[18]

One possible explanation for the observed decrease in the signal intensity is that the tautomerization of the dihydropyridazine intermediate affects the fluorescence of the coumarin dyes. To validate this hypothesis, we followed the reaction progress by monitoring changes in the fluorescent signal over 2 hours. We used lower excess of the dienophile in this case to ensure convenient monitoring of the otherwise fast reaction. To suppress possible tautomerization of the dihydropyridazine intermediates promoted by the free hydroxyl group of the axial TCO-OH, we used another TCO derivative that incorporates axial TCO attached to a short PEG_3 moiety (TCO-PEG) through a carbamate linker. These experiments revealed that after initial increase in the fluorescence, the signal intensity of the click products formed with the TCO-PEG dienophile decreases considerably (Figure 2 and Figure S5).

The only exceptions were compounds **1a–d**, which showed no or only a slight decrease in the signal intensity. Under the same reaction conditions, all tetrazines showed an increase in the fluorescence signal with the BCN which remains constant over the time course (Figure 2 and Figure S5). Although these experiments did not afford a clear explanation how and why the signal intensity decreases with the TCO, they do demonstrate that the structure of the central dihydropyridazine core plays an important role in defining the photophysical properties of the dyes.

Previous studies have shown that incorporation of the azetidine moiety into the structure of various dyes can significantly improve their fluorescence quantum yield (Φ).[19] The N,N-dimethylpiperazin-1-ium moiety was used for similar purposes.[20] In line with these studies, one of our goals was to investigate the influence of these moieties on the Φ of the fluorogenic

Coum-Tz probes.[21] We determined the Φ for several dyes formed in reaction of these probes with the BCN dienophile. It is important to note that similar experiments with the TCO dienophile are basically impossible as the fluorescence of these dyes is changing in time (Figure S5). By using quinine sulfate as the reference standard,[22] we could confirm improved Φ in several cases (Table 1). For example, by comparing the Φ value of compounds **1j** with that of **1f** and **1g** it is obvious that the introduction of the azetidine moiety leads to a ca. 3-fold increase in the fluorescence quantum yield in favor of the latter compounds. Similarly, alkylation of methylpiperazine **1l** yields compound **1n** having 1.5-fold higher Φ value. These data clearly show that the azetidine- and N,N-dimethylpiperazin-1-ium-substituted coumarins are preferable in this regard.

The prevailing explanation of the quantum-yield enhancement is based on the expectation that the azetidine or dimethylpiperazinium substituents suppress the formation of twisted intramolecular charge transfer (TICT) upon photoexcitation.[20b, 23] The TICT form relaxes without emission of a photon, which leads to non-radiative decay of the photoexcited state and lower Φ. In the TICT form, the electron-donating moiety (e.g., the azetidine ring) is in a nearly perpendicular arrangement with respect to the planar fluorophore skeleton. This arrangement leads to the formation of a charge-separated species. However, an alternative explanation of the increase of quantum yields of azetidinyl-substituted coumarins was proposed recently.[24] It was shown that hydrogen bonding with solvent water molecules was the prominent deactivation pathway, which was inhibited by the substitution with an azetidinyl ring.

DFT calculations

In an attempt to explain the observed Φ enhancement for the Coum-Tz derivatives and to confirm/disprove the participation of the TICT form, we performed a computational study at the density functional theory (DFT) level. First, we performed geometry optimization of the ground-state structures and a potential-energy scan corresponding to the rotation of the azetidinyl and piperazinyl substituent. The C—N bond lengths between the coumarin skeleton and the substituent and the estimated barriers of rotation around the C—N bond are almost identical for both the TCO and BCN derivatives (Table 2). The maxima on the potential-energy scan always correspond to a perpendicular arrangement of the nitrogen-containing ring and the coumarin plane. Then, the same geometry optimization and potential-energy scan were performed for first excited
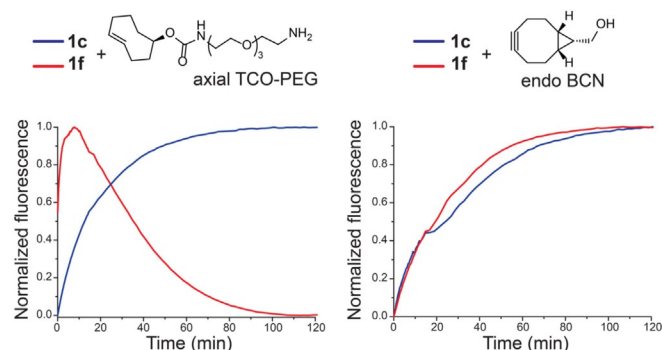

Figure 2. Example of the experiment showing changes in the fluorescence signal for reaction of tetrazines **1c** and **1f** with the TCO-PEG and BCN dienophiles. Normalized fluorescence is shown. See Figure S5 for the rest of tetrazines.

Table 2. The calculated C—N bond lengths (Å) and rotational barriers (kcal mol^{-1}) around the C—N bond estimated from the potential-energy scan.

Ground state	d(C—N)	ΔE	Excited state	d(C—N)	ΔE
BCN-azet	1.372	9.1	BCN-azet	1.375	7.9
BCN-pip-neut	1.399	7.4	BCN-pip-neut	1.398	3.7
BCN-pip-ion	1.431	1.0	BCN-pip-ion	1.431	0.9

Chemistry–A European Journal

Full Paper
doi.org/10.1002/chem.202001290

Chemistry Europe
European Chemical
Societies Publishing

states of the molecules and the results are similar to those for the ground states. Structures with perpendicular arrangement of the azetidinyl/piperazinyl ring, that is, those corresponding to the TICT states, have always the highest energy in the potential-energy scan.

In a very recent computational study, the importance of the solvation model for accurate computations of TICT forms has been pointed out.[25] Therefore, we re-optimized the tentative TICT structures with a SMD model used for implicit water solvation. However, these geometry optimizations always led to structures close to the ground-state structures with minimal energy, that is, the TICT structures are not stable.

In summary, our computational study did not confirm the existence of the TICT structures in the coumarin derivatives. Therefore, the participation of intermolecular hydrogen bonds on the non-radiative deactivation pathway seems to be more probable.

Cellular imaging experiments

Encouraged by the excellent turn-on properties of the Coum-Tz probes, we aimed to investigate their suitability for cellular imaging experiments. With the goal of identifying the best performing derivatives, we first carried out a series of preselection experiments. We modified fixed and permeabilized retinal pigment epithelium (RPE) cells with axial TCO-PEG$_3$ or *endo* BCN-PEG$_3$ *N*-hydroxysuccinimide esters to introduce the dienophiles onto cells. After the reaction with a pool of thirteen tetrazines, we analyzed the click-modified cells by fluorescence-activated cell sorting (FACS) (Figure 3, Figure S9).

As expected, all tetrazines showed significant shift in the fluorescence intensity after the click reaction, which is in good agreement with the light-up experiments performed before in the cuvette. We could also confirm higher turn-on ratios in the reaction of the tetrazines with the BCN dienophile-modified cells. Importantly, the fluorescent signal in cells treated only with the Coum-Tz probes without modification with the dienophile was significantly reduced. For practical reasons, these experiments were performed without extra purification steps of the coumarin probes.

To further evaluate our probes for application in cell imaging we prepared TCO- and BCN-containing wheat germ agglutinin (WGA) conjugates (Supporting Information). WGA is a lectin t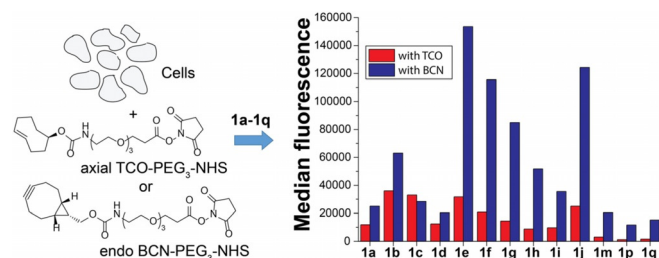hat binds *N*-acetyl-β-D-glucosamine residues present on the cell-surface glycoconjugates. In this experiment, fixed and permeabilized cells were incubated with the dienophile-modified WGA and were subsequently treated with the same pool of Coum-Tz compounds to initiate the fluorogenic reaction. As in the previous case, the cells were analyzed by FACS to enable a quantitative comparison (Figure 4, Figure S9).
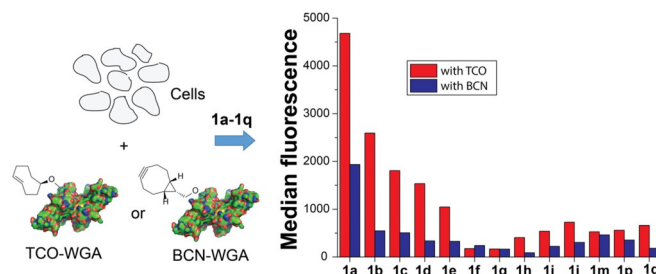

Figure 4. Results from FACS analysis of U2OS cells treated with TCO- or BCN-containing WGA followed by fluorogenic labeling using the indicated Coum-Tz probes. WGA structure was created from the available crystal structure of the protein (PDB 1WGT). Excitation: 405 nm; Emission: 525 ± 50 nm.

In addition, we performed the same experiment on live cells and inspected the cells on a confocal scanning microscope to verify the cellular localization of the click products (Figure S10). These experiments confirmed successful click labeling of the cell surface. However, we noticed significant differences in performance of the individual tetrazines in this case. Surprisingly, compound **1a** gave the best turn-on response in this experiment as was obvious from both FACS analysis and from the confocal scanning microscope images. In addition, the TCO-modified WGA-labeled cells were more fluorescent when compared to the BCN-WGA treated cells, which is contrary to our results obtained in the cuvette. The majority of the tetrazine probes showing excellent turn-on values in all previous experiments gave relatively weak staining in this case.

One possible reason for these observations can be in that the tetrazines react with the dienophile at different rates. Therefore, we determined the second order rate constant of the reaction of tetrazines **1a**, **c**, **d**, **f** and **1g** with BCN (Figure S7). Indeed, these measurements confirmed that tetrazine **1a** is about 45 times more reactive when compared to for example, tetrazine **1f** ($k_2 = 1400 \pm 60$ M^{-1}s^{-1} vs. 29 ± 1 M^{-1}s^{-1} at 37 °C in PBS). It is known that tetrazines react in most cases with the TCO more rapidly when compared to the BCN.[26] Therefore, the fact that the fluorogenic reaction on the cells with the TCO-modified WGA gave in all cases better signal further highlights the importance of reaction kinetics in the experiment. On the other hand, tetrazine **1d** is the most reactive among the series ($k_2 = 4000 \pm 400$ M^{-1}s^{-1}) indicating that there are possibly other factors which influence the fluorogenic reaction when performed in/on cells.[27] For example, the lipophilicity and with that associated better cell permeability can be important (Table S2).

The above experiments were mainly carried out on fixed and permeabilized cells and served as a guide for preselection

Figure 3. Results from FACS analysis of RPE cells modified with TCO or BCN dienophiles followed by fluorogenic labeling using the indicated Coum-Tz probes. Excitation 405 nm, Emission 525 ± 50 nm.

Chemistry–A European Journal

Full Paper
doi.org/10.1002/chem.202001290

Chemistry Europe
European Chemical
Societies Publishing

of the best performing tetrazines. The main advantage of bio-orthogonal probes is in their compatibility with live systems. We therefore turned our attention to live cell imaging and performed a series of experiments with compounds **1a**, **c**, **d** and **1f**. We chose two types of probes to evaluate the tetrazines in different cellular compartments. First, we prepared a TCO- and BCN-functionalized, microtubule-binding anticancer agent docetaxel (TCO-docetaxel and BCN-docetaxel, see Supporting Information for the synthesis) and second, we attached the TCO or BCN to triphenylphosphonium moiety, which is able to transport the compounds to mitochondria.[28]

To compare the four tetrazines, we incubated live HeLa cells with a 1 μm TPP-TCO, TPP-BCN or TCO-docetaxel and BCN-docetaxel and added 1 μm solution of freshly purified tetrazines **1a**, **c**, **d** and **1f**. As a control, the cells were treated with the tetrazines in the absence of the dienophile-containing compounds. The cells were then imaged on confocal scanning microscope. As observed in experiment with WGA-modified cells, compounds **1a** and **1c** outperformed in labeling the other two tetrazines. Importantly, there was no background signal in control cells treated with the tetrazines alone, confirming the excellent turn-on properties of the fluorogenic probes. No additional washing steps after tetrazine addition were required (Figure 5).

This experiment shows that **1c** yields brighter signal than does **1a** in combination with TPP-BCN. However, the latter compound is better on average and showed superior labeling in all cases including the WGA labeling experiment. The only exception was docetaxel-BCN, where no labeling with any of

the four tetrazines was observed under these experimental conditions. It seems that certain Coum-Tz structures may have preference for particular cellular compartment and/or form brighter dyes in combination with particular dienophile in the cells within this compartment (Figure S11). Steric reasons can also play an important role (e.g., shielding of the dienophile when docetaxel binds to microtubules).

To better understand the difference in labeling efficiency of tetrazines **1a** and **1f**, we added to cells incubated with the TCO-TPP the latter compound at various concentrations. As can be seen from Figure 6, even 25 μm concentration of **1f** did not yield better labeling signal. These experiments demonstrate that even though compound **1a** does not light-up as strongly as does compound **1f** (Table 1), it outperforms the latter compound significantly in cellular experiments. It is important to note that the observed decay in the fluorescent signal (Figure 2, Figure S5) of the click product in this case is not responsible for the observed lower signal intensity. The experiment was performed on a time scale where this effect is not pronounced and the signal in **1f** treated cells was stable during the experiment.

Thrilled by the superior performance of compound **1a** we next performed a series of experiments in two additional cell lines. The live cells were first treated with 1 μm TPP-TCO or docetaxel-TCO. They were washed to remove excess of the compounds and were then incubated with 1 μm **1a**. We observed formation of a specific fluorescent signal in all cell lines. As in all previous cases, there was no background signal in cells treated only with **1a**, and no additional washing steps were required after tetrazine addition, thus demonstrating excellent turn-on properties of the compound (Figure 7).

To demonstrate the efficiency of the compound for live cell labeling application we next performed a series of time-lapse experiments. We added tetrazine **1a** to cells pre-treated with the TPP-TCO compound, docetaxel-TCO or WGA-TCO directly under the microscope. Clear fluorescent signal developed in the cells within tens of seconds and remained stable thereafter (Supporting Videos 1–3). These experiments clearly show the superior performance of the compound and highlight its high reactivity and excellent turn-on properties in cellular imaging experiments.
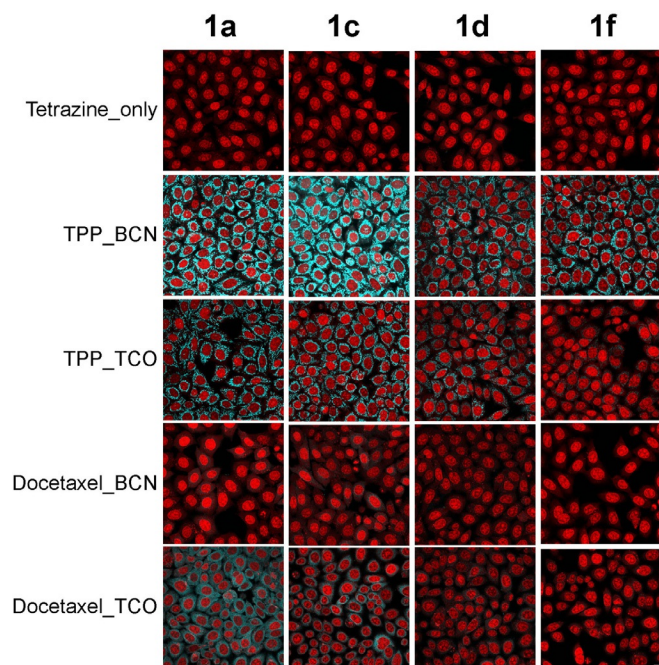

Figure 5. Confocal microscope images showing comparison of four tetrazines (cyan color) in live cell fluorogenic labeling using the mitochondrion-selective TPP probes and microtubule-binding docetaxel. All compounds were used at 1 μm concentration. DRAQ5 was used for nuclear staining. Scale bar 10 μm. Excitation (coumarin): 405 nm; emission: 438–499 nm; excitation (DRAQ5): 633 nm; emission: 639–691 nm.
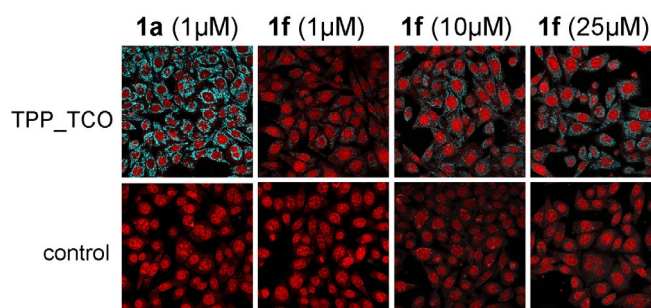

Figure 6. Comparison of cell labeling using 1 μm **1a** and different concentrations of compound **1f** in live HeLa cells. TCO-TPP was added at 1 μm final concentration. DRAQ5 was used for nuclear staining. Scale bar 10 μm. Excitation (coumarin): 405 nm; emission: 438–499 nm; excitation (DRAQ5): 633 nm; emission: 639–691 nm.
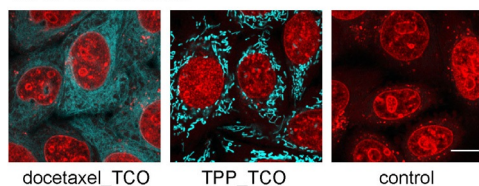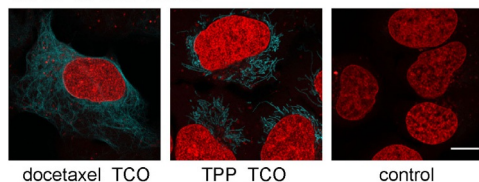
Chemistry–A European Journal

Full Paper
doi.org/10.1002/chem.202001290

Chemistry Europe
European Chemical
Societies Publishing

1a in HeLa cells

docetaxel_TCO   TPP_TCO   control

1a in U2OS cells

docetaxel_TCO   TPP_TCO   control

1a in A549 cells

docetaxel_TCO   TPP_TCO   control

Figure 7. Images from confocal scanning microscope showing live cell no-wash fluorogenic labeling using coumarin-tetrazine **1a** in different cell lines. The cells were first treated with 1 μm docetaxel-TCO or TPP-TCO and then with 1 μm **1a**. DRAQ5 was used for nuclear staining. Scale bar 10 μm. Excitation (coumarin): 405 nm; emission: 438–499 nm; excitation (DRAQ5): 633 nm; emission: 639–691 nm.
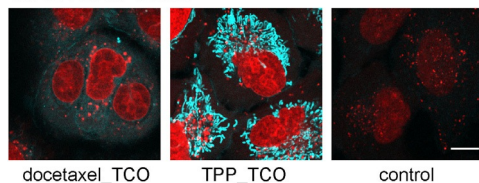
Conclusions

In summary, we have systematically studied the photophysical properties of a series of seventeen coumarin–tetrazine probes that light-up and produce fluorophores upon reaction with TCO- and BCN-containing molecules. Our study shows that the attachment of azetidine or *N,N*-dimethylpiperazine moiety to the coumarin scaffold yields compounds with improved fluorescence quantum yield. Our computational study could not confirm the TICT as the main mechanism responsible for this enhancement. The fluorescence turn-on properties of the probes are in general excellent, but depend on the substituents attached to the tetrazine core. Our labeling experiments revealed several probes having excellent properties for application in bioimaging. Among these, dye comprising of an azetidine coumarin connected through a pyridyl linker to 6-pyrimidine-substituted tetrazine (**1a**) was identified as the most versatile probe that repeatedly showed superior labeling efficiency in live cells. Although the origin of this excellent performance is not completely clear at the moment, we speculate that it is a combination of good reaction kinetics and cell permeability which makes the compound so unique. The information provided in this study could serve as a valuable guideline for the future development of fluorescence turn-on probes based on the coumarin scaffold. Importantly, it also demonstrates that a high fluorescence turn-on ratio is not the only measure of good quality probes, but that other factors must

be considered when designing fluorogenic bioorthogonal probes for bioimaging applications.

Conflict of interest

The authors declare no conflict of interest.

Keywords: click chemistry · coumarins · fluorescence · live cell bioimaging · tetrazines

[1] a) I. Sarkar, A. K. Mishra, *Appl. Spectrosc. Rev.* **2018**, *53*, 552–601; b) L. H. Qin, W. Hu, Y. Q. Long, *Tetrahedron Lett.* **2018**, *59*, 2214–2228; c) M. King, A. Wagner, *Bioconjugate Chem.* **2014**, *25*, 825–839; d) M. F. Debets, J. C. M. van Hest, F. P. J. T. Rutjes, *Org. Biomol. Chem.* **2013**, *11*, 6439–6455; e) J. M. Baskin, C. R. Bertozzi, *Qsar Comb. Sci.* **2007**, *26*, 1211–1219.

[2] a) F. de Moliner, N. Kielland, R. Lavilla, M. Vendrell, *Angew. Chem. Int. Ed.* **2017**, *56*, 3758–3769; *Angew. Chem.* **2017**, *129*, 3812–3823; b) L. Wang, M. S. Frei, A. Salim, K. Johnsson, *J. Am. Chem. Soc.* **2019**, *141*, 2770–2781; c) P. F. Liu, X. Y. Mu, X. D. Zhang, D. Ming, *Bioconjugate Chem.* **2020**, *31*, 260–275; d) E. A. Specht, E. Braselmann, A. E. Palmer, *Annu. Rev. Physiol.* **2017**, *79*, 93–117; e) Y. H. Fu, N. S. Finney, *Rsc Adv.* **2018**, *8*, 29051–29061.

[3] a) T. Nagano, *P. Jpn. Acad. Ser. B* **2010**, *86*, 837–847; b) Z. Q. Guo, S. Park, J. Yoon, I. Shin, *Chem. Soc. Rev.* **2014**, *43*, 16–29; c) H. M. Shang, H. Chen, Y. H. Tang, Y. Y. Ma, W. Y. Lin, *Biosens. Bioelectron.* **2017**, *95*, 81–86.

[4] H. L. Li, J. C. Vaughan, *Chem. Rev.* **2018**, *118*, 9412–9454.

[5] a) A. Nadler, C. Schultz, *Angew. Chem. Int. Ed.* **2013**, *52*, 2408–2410; *Angew. Chem.* **2013**, *125*, 2466–2469; b) E. Kozma, P. Kele, *Org. Biomol. Chem.* **2019**, *17*, 215–233.

[6] a) E. Kozma, O. Demeter, P. Kele, *ChemBioChem* **2017**, *18*, 486–501; b) E. Németh, G. Knorr, K. Németh, P. Kele, *Biomolecules* **2020**, *10*, 397.

[7] N. K. Devaraj, S. Hilderbrand, R. Upadhyay, R. Mazitschek, R. Weissleder, *Angew. Chem. Int. Ed.* **2010**, *49*, 2869–2872; *Angew. Chem.* **2010**, *122*, 2931–2934.

[8] a) J. C. T. Carlson, L. G. Meimetis, S. A. Hilderbrand, R. Weissleder, *Angew. Chem. Int. Ed.* **2013**, *52*, 6917–6920; *Angew. Chem.* **2013**, *125*, 7055–7058; b) D. Wu, D. F. O'Shea, *Chem. Commun.* **2017**, *53*, 10804–10807.

[9] a) H. X. Wu, J. Yang, J. Seckute, N. K. Devaraj, *Angew. Chem. Int. Ed.* **2014**, *53*, 5805–5809; *Angew. Chem.* **2014**, *126*, 5915–5919; b) A. Wieczorek, P. Werther, J. Euchner, R. Wombacher, *Chem. Sci.* **2017**, *8*, 1506–1510; c) E. Kozma, G. E. Girona, G. Paci, E. A. Lemke, P. Kele, *Chem. Commun.* **2017**, *53*, 6696–6699; d) G. Beliu, A. J. Kurz, A. C. Kuhlemann, L. Behringer-Pliess, M. Meub, N. Wolf, J. Seibel, Z. D. Shi, M. Schnermann, J. B. Grimm, L. D. Lavis, S. Doose, M. Sauer, *Commun. Biol.* **2019**, *2*, 261; e) A. Wieczorek, T. Buckup, R. Wombacher, *Org. Biomol. Chem.* **2014**, *12*, 4177–4185.

[10] G. Knorr, E. Kozma, J. M. Schaart, K. Nemeth, G. Torok, P. Kele, *Bioconjugate Chem.* **2018**, *29*, 1312–1318.

[11] L. G. Meimetis, J. C. Carlson, R. J. Giedt, R. H. Kohler, R. Weissleder, *Angew. Chem. Int. Ed.* **2014**, *53*, 7531–7534; *Angew. Chem.* **2014**, *126*, 7661–7664.

[12] a) Y. Qu, P. Pander, O. Vybornyi, M. Vasylieva, R. Guillot, F. Miomandre, F. B. Dias, P. Skabara, P. Data, G. Clavier, P. Audebert, *J. Org. Chem.* **2020**, *85*, 3407–3416; b) Y. Lee, W. Cho, J. Sung, E. Kim, S. B. Park, *J. Am. Chem. Soc.* **2018**, *140*, 974–983.

Chemistry–A European Journal

Full Paper
doi.org/10.1002/chem.202001290

Chemistry Europe
European Chemical
Societies Publishing

[13] a) A. Vázquez, R. Dzijak, M. Dracinsky, R. Rampmaier, S. J. Siegl, M. Vrabel, *Angew. Chem. Int. Ed.* **2017**, *56*, 1334–1337; *Angew. Chem.* **2017**, *129*, 1354–1357; b) X. Shang, X. Song, C. Faller, R. Lai, H. Li, R. Cerny, W. Niu, J. Guo, *Chem. Sci.* **2017**, *8*, 1141–1145; c) S. J. Siegl, J. Galeta, R. Dzijak, A. Vazquez, M. Del Rio-Villanueva, M. Dracinsky, M. Vrabel, *ChemBioChem* **2019**, *20*, 886–890.

[14] Y. Y. Qu, F. X. Sauvage, G. Clavier, F. Miomandre, P. Audebert, *Angew. Chem. Int. Ed.* **2018**, *57*, 12057–12061; *Angew. Chem.* **2018**, *130*, 12233–12237.

[15] P. Agarwal, B. J. Beahm, P. Shieh, C. R. Bertozzi, *Angew. Chem. Int. Ed.* **2015**, *54*, 11504–11510; *Angew. Chem.* **2015**, *127*, 11666–11672.

[16] S. J. Siegl, R. Dzijak, A. Vazquez, R. Pohl, M. Vrabel, *Chem. Sci.* **2017**, *8*, 3593–3598.

[17] a) M. Bojtár, A. Kormos, K. Kis-Petik, M. Kellermayer, P. Kele, *Org. Lett.* **2019**, *21*, 9410–9414; b) Y. W. Jun, H. R. Kim, Y. J. Reo, M. Dai, K. H. Ahn, *Chem. Sci.* **2017**, *8*, 7696–7704.

[18] a) X. Fan, Y. Ge, F. Lin, Y. Yang, G. Zhang, W. S. Ngai, Z. Lin, S. Zheng, J. Wang, J. Zhao, J. Li, P. R. Chen, *Angew. Chem. Int. Ed.* **2016**, *55*, 14046–14050; *Angew. Chem.* **2016**, *128*, 14252–14256; b) J. C. T. Carlson, H. Mikula, R. Weissleder, *J. Am. Chem. Soc.* **2018**, *140*, 3603–3612; c) R. M. Versteegen, W. Ten Hoeve, R. Rossin, M. A. R. de Geus, H. M. Janssen, M. S. Robillard, *Angew. Chem. Int. Ed.* **2018**, *57*, 10494–10499; *Angew. Chem.* **2018**, *130*, 10654–10659; d) R. M. Versteegen, R. Rossin, W. ten Hoeve, H. M. Janssen, M. S. Robillard, *Angew. Chem. Int. Ed.* **2013**, *52*, 14112–14116; *Angew. Chem.* **2013**, *125*, 14362–14366.

[19] a) J. B. Grimm, A. K. Muthusamy, Y. Liang, T. A. Brown, W. C. Lemon, R. Patel, R. Lu, J. J. Macklin, P. J. Keller, N. Ji, L. D. Lavis, *Nat. Methods* **2017**, *14*, 987–994; b) J. B. Grimm, B. P. English, J. Chen, J. P. Slaughter, Z. Zhang, A. Revyakin, R. Patel, J. J. Macklin, D. Normanno, R. H. Singer, T. Lionnet, L. D. Lavis, *Nat. Methods* **2015**, *12*, 244–250.

[20] a) Z. Ye, W. Yang, C. Wang, Y. Zheng, W. Chi, X. Liu, Z. Huang, X. Li, Y. Xiao, *J. Am. Chem. Soc.* **2019**, *141*, 14491–14495; b) X. Lv, C. Gao, T. Han, H. Shi, W. Guo, *Chem. Commun.* **2020**, *56*, 715–718.

[21] a) O. Morawski, L. Kielesinski, D. T. Gryko, A. Sobolewski, *Chem. Eur. J.* **2020**, *26*, 7281–7291; b) S. Singha, D. Kim, B. Roy, S. Sambasivan, H. Moon, A. S. Rao, J. Y. Kim, T. Joo, J. W. Park, Y. M. Rhee, T. Wang, K. H. Kim, Y. H. Shin, J. Jung, K. H. Ahn, *Chem. Sci.* **2015**, *6*, 4335–4342.

[22] C. Würth, M. Grabolle, J. Pauli, M. Spieles, U. Resch-Genger, *Nat. Protoc.* **2013**, *8*, 1535–1550.

[23] X. Liu, Q. Qiao, W. Tian, W. Liu, J. Chen, M. J. Lang, Z. Xu, *J. Am. Chem. Soc.* **2016**, *138*, 6960–6963.

[24] G. Bassolino, C. Nancoz, Z. Thiel, E. Bois, E. Vauthey, P. Rivera-Fuentes, *Chem. Sci.* **2018**, *9*, 387–391.

[25] C. Wang, Q. L. Qiao, W. J. Chi, J. Chen, W. J. Liu, D. Tan, S. McKechnie, D. Lyu, X. F. Jiang, W. Zhou, N. Xu, Q. S. Zhang, Z. C. Xu, X. G. Liu, *Angew. Chem. Int. Ed.* **2020**, *59*, 10160–10172; *Angew. Chem.* **2020**, *132*, 10246–10258.

[26] a) R. Selvaraj, J. M. Fox, *Curr. Opin. Chem. Biol.* **2013**, *17*, 753–760; b) D. Z. Wang, W. X. Chen, Y. Q. Zheng, C. F. Dai, K. Wang, B. W. Ke, B. H. Wang, *Org. Biomol. Chem.* **2014**, *12*, 3950–3955.

[27] O. Vakuliuk, Y. W. Jun, K. Vygranenko, G. Clermont, Y. J. Reo, M. Blanchard-Desce, K. H. Ahn, D. T. Gryko, *Chem. Eur. J.* **2019**, *25*, 13354–13362.

[28] M. P. Murphy, *BBA-Bioenergetics* **2008**, *1777*, 1028–1031.